Improving the Wave Energy production using multi-size WEC arrays with Passive Control

Alday Gonzalez, Matias; Raghavan, Vaibhav; Lavidas, George

DOI
10.1115/OMAE2024-123655

Publication date
2024

Document Version
Final published version

Published in
Ocean Renewable Energy

Proceedings of the OMAE 2024
International Conference on Ocean, Offshore & Arctic Engineering
OMAE2024
June 9–June 14, 2024, Singapore Expo, Singapore

OMAE2024-123655

IMPROVING THE WAVE ENERGY PRODUCTION USING MULTI-SIZE WEC ARRAYS WITH PASSIVE CONTROL

Matias Alday G.[1,*], Vaibhav Raghavan[1], George Lavidas[1]

[1]Marine Renewable Energies Lab, Delft University of Technology, Delft, Netherlands

ABSTRACT

One of the key aspects to consider before large scale deployments of wave energy converters (WEC), is to optimize the devices' characteristics to improve wave power absorption. Typically, devices with passive control are designed to have the highest efficiency in wave power absorption/production in the range of the most frequent wave conditions. In general, there is an intrinsic "trade-off" between the range of wave conditions where a WEC can operate and the operation efficiency which, in the end, is linked to the energy production yield. Outside the most frequent wave conditions, there is still a non-negligible percentage of occurrences of more energetic sea states carrying high energy flux values. Given the specific design characteristics of a WEC device, lower operation efficiency is expected during these stronger sea states, which is translated as a lower production compared to the available (usable) resource. In the present study, a multi-size point absorber WEC array, using passive internal control, is proposed to optimize wave power production at the array level. The main aim of this work is to verify the combined use of devices designed to work in the most frequent wave conditions, with WECs which mass and dimensions are defined to improve their response during stronger sea states. A comparison of the mean produced power is performed between a proposed multi-array and a single size one. This is done using 30 years of spectral wave data obtained from an implementation of the WAVEWATCH III model, while response of the wave energy converters array is simulated with the boundary element model HAMS-MREL. Preliminary results, using 10-devices arrays, show a promising increase in production from 60 to 140% when larger WECs are included.

Keywords: Wave Energy, WEC farms, HAMS-MREL, Sea states

1. INTRODUCTION

The increasing efforts to reduce the use of fossil fuels have led to a continuous search of alternative energy sources. In the last 2 decades, special interest has been put in the marine environment. Particularly, the wave resource has been one of the most studied alternatives given its global abundance [1]. As a result, a large amount of publications have been carried out with aims to characterize it, quantify it, and define potential sites for extraction in different parts of the world [e.g.; 2–7].

With the increasing understanding of the wave resource, many different concepts to extract energy from the waves have been developed, tested and analyzed over the years as technology advances [8–11]. As part of the "technology journey" of a wave energy converter (WEC), it is required to pass the stages of proof of viability and scaleability to reach the proof of durability phase. This latter one implies the implementation of first WEC farms prior to market diffusion [9]. In this sense, it is understood that to produce a commercially attractive amount of MW adequate for even power distribution, the design of a WEC farm requires many units [12, 13]. Furthermore, in order to maximize wave energy absorption/conversion, at a specific site, the characteristics of the devices should be optimized.

Basically, the initial design (mainly size and mass) of a WEC typically aims to provide the best performance for the most common wave conditions. At this stage, it is expected that the power take-off (PTO) of the device is more efficient for a narrow range of wave periods. Nowadays the efficiency of the WEC's operation range is typically extended by including PTO passive or active response controls [e.g.; 14–17]. In fact, the used control strategy can be considered one of the main elements determining the efficiency of the system [16]. Although the development of active (or reactive) controls have shown an increase of energy extraction from waves, the overall higher usage of energy from the system can significantly affect the efficiency. On the other hand, the implementation of a passive control is technically simpler (and cheaper), and it can effectively decrease the peak to mean produced power ratio [18].

Outside the range of the most frequent wave conditions, there is still a non-negligible occurrence of stronger sea states. These ones typically present larger significant wave heights (H_s) and longer peak periods (T_p), carrying high energy flux values. The

*Corresponding author: M.F.AldayGonzalez@tudelft.nl
Documentation for `asmeconf.cls`: Version 1.35, June 25, 2024.

main objective of the present study is to evaluate the effects of having multi-size WEC farms to improve production during more energetic sea states. To this aim, the estimated production of a single-size farm with devices designed to work in the most frequent wave conditions is compared to a multi-size WEC farm. The estimations are done with numerical simulations of point absorber's arrays using the in-house boundary element model HAMS-MREL. In this case, 2 locations with different wave climate characteristics are selected to perform the analysis: Ireland (North Atlantic) and The Netherlands (North Sea). The 30 years spectral wave data used in the analysis, is taken from an implementation of the WAVEWATCH III [WW3; 19, 20] model specially adjusted for the areas of interest. The use of local detailed spectral data, instead of parametric spectral shapes (e.g.; JONSWAP) which typically do not capture bi-modal sea states, has a large impact on the absorbed power estimations. The proposed approach helps to improve the accuracy of the WEC response simulations in the frequency domain.

In the present paper, the method and materials are presented in section 2, which includes a brief description on the HAMS-MREL and WW3 models implementation. Then, results and discussions are presented in section 3, followed by the conclusions in section 4.

2. METHOD AND MATERIALS

2.1 Hydrodynamic model of the Wave Energy farm based on the Converter Corpower C4 devices

This section briefly describes the hydrodynamic modelling of the wave energy farm consisting of the Corpower C4 wave energy devices. A linearized sub-optimal array power matrix considering viscous losses is derived here, which is used to estimate the power produced at a specific site.

It should be highlighted that the simulated WECs are based in the geometry and size/mass of the C4. It is important to notice that not all characteristics of the C4 are incorporated in the BEM model simulations.

2.1.1 Device Description. The Corpower C4 device (shown in Fig. 1) is a point absorber wave energy converter [21]. The C4 is selected for this analysis since it is currently one of the state-of-the-art devices, and close to achieve commercialisation. Two interesting features of the device are: 1) Wave-spring system [22] which amplifies the motion and power capture of the device by providing a negative spring function, 2) Pre-tensioning system which replaces some of the mass otherwise needed to balance the buoyancy effect and a composite spherical buoy hull structure, that provides high volume with low mass. These elements have not been included in the numerical simulations at this stage of the study.

The device is anchored to the bottom and employs real-time control algorithms to maximize its power output. The draft of 6 m was assumed by the authors for this study and the natural frequency was calculated based on the aforementioned properties for the single device.

2.1.2 Equations of motion. A frequency domain model was used for estimating the response of the devices in wave farms, considering the interactions between them. Only heave motion

FIGURE 1: Corpower C4 Wave Energy Converter Device [21]

TABLE 1: Properties of the Corpower C4 device

Property	Value	Unit
Diameter	9	m
Height	18	m
Installation depth (minimum)	40	m
Weight	70	tonne
Bouy Draft	6	m
Undamped Natural period (heave)	3	s

was considered here. The coupled equations of motion were derived and solved simultaneously. If we consider N devices in the farm, the general equation of motion for the p^{th} device can be given as:

$$[-\omega^2(m_d^p) + i\omega(b_{PTO}^p + b_v^p) + c_h^p + \Sigma_{q=1}^{N}(-\omega^2 m_{33}^{(p)(q)} + i\omega b_{33}^{(p)(q)})]s = f_3^p$$

where ω is the incident wave frequency, m_d^p is the mass of the p^{th} device, b_{PTO}^p is the PTO (Power Take Off) coefficient of the p^{th} device, b_v^p is the linearized viscous damping coefficient of the p^{th} device, c_h^p is the hydro-static stiffness coefficient in heaving of the p^{th} device, f_e^p is the heave exciting force of the p^{th} device, $m_{33}^{(p)(q)}$ and $b_{33}^{(p)(q)}$ are the added mass and radiation damping respectively of the p^{th} device in heave due to the motion of the q^{th} device in heaving. s is the displacement amplitude of the device also referred to as the body excursion. When the amplitude of the incident wave is 1 m, then s represents the RAO (Response

amplitude Operator) in heave motion for the device.

Within the scope of this formulation, the following interactions have not been considered - (i) the wave spring component of the device which provides a negative spring stiffness and (ii) the pre-tensioning mechanism (iii) the moorings, as the device is anchored to the seabed directly. The PTO damping is then calculated based on the work of Hals et.al. [23]. For most practical cases, the PTO reactance is negligible or zero and so considering just the PTO damping condition would be sufficient [24]. Therefore, a sub-optimal passive control has been incorporated within the PTO damping coefficient, based on the formulation which takes into account the losses due to viscosity. To determine the viscous losses, a linearized approach has been used.

2.1.3 BEM model. The frequency dependent hydrodynamic coefficients and exciting forces are obtained from the in-house newly developed frequency domain Boundary Element Method (BEM) solver HAMS-MREL (work showcasing its methodology and validation is currently under review in 'Applied Ocean Research'). This solver is built upon the existing open-source BEM solver HAMS developed by Y. Liu [25]. Shallow water conditions were assumed since the considered depth is 25 m at the location in the North Sea and intermediate water depth conditions were considered for Ireland. The mesh taken is from an earlier study done by the authors [26]. Convergence studies were done as part of that research.

2.1.4 Natural frequency of the devices in farms. The natural frequencies of the devices within a farm configuration were obtained considering all inter-device interactions. The coefficients for both the diagonal and off-diagonal terms in the radiation damping matrix were found to be well below the critical damping of the individual devices considering the Mass and Stiffness (hydrostatic) matrices, and were therefore not considered in the computation of the natural frequency of the devices. The undamped natural frequencies were thus estimated by an iterative process since the added mass coefficients for all the devices are dependent on the incident wave frequency ω. For every incident wave frequency, the eigen values of the matrix $M^{-1}K$ are obtained, where M is fully populated mass matrix and K is the diagonal hydrostatic stiffness matrix. The positive root of the eigen value gives the frequency, which should then be matched with the incident wave frequency to obtain the natural frequency. This process is performed for each device to get its natural frequency which can then be used in the estimation of the linearized viscous losses.

2.1.5 Sub-optimal PTO control and viscous losses. The obtained natural frequency of each device is used to estimate the linearized viscous losses using the Lorentz linearization approach ([27, 28]). The maximum heave displacement of all devices is assumed to be $0.6a$ where a is the radius of the bouy and is applied as a displacement constraint. Sub-optimal passive control including viscous losses was incorporated based on the work of Hals et al. [23] which considers the displacement constraint when obtaining the optimized PTO coefficient. It should be noted that inter-device added mass and radiation damping coefficients (off-diagonal elements of the added mass and radiation damping matrix) are not considered for this calculation.

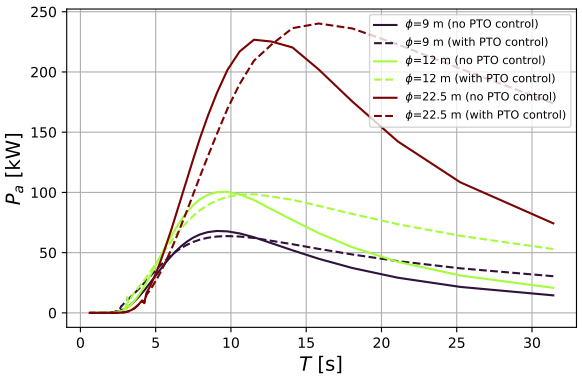

FIGURE 2: Single WEC absorbed power estimations. Point absorbers with diameters of 9, 12 and 22.5 m, and mass of 70000, 175000 and 280000 kg respectively. All simulations use a 1 m wave height.

2.2 Power Estimation and Array Power Matrices

The average power produced by the WEC over various sea states is quantified in a power matrix. For its computation, irregular wave sea states based on the significant wave height H_s and peak period T_p are considered. From the wave data for the given location, the spectra are derived directly from the MREL dataset per sea state, which can then be used to compute the significant heave amplitude ($\overline{z}_{a_{1/3}}$) and average zero-crossing period (T_{2z}). The methodology is explained in detail in our previous work [26].

When deriving the power matrices, the spectra obtained from the MREL wave hindcast as well as the JONSWAP spectra is used. For sea states that do not occur at the given location, the JONSWAP spectra is used to derive the average power. For sea states that do occur, the spectra is derived from the MREL dataset. With this procedure, we have a fully populated power matrix that also considers the characteristics of the sea states at the assessment location.

The array power matrices are derived by adding the average power per sea state from all devices in a given farm configuration. The power matrices are capped to $H_s \leq 9$ m.

2.3 Analyzed WEC farms characteristics

The main idea behind increasing the size and mass of a wave energy converter, is to shift its natural frequency towards longer periods (lower frequencies). Thus, it is expected that the device will be more "efficient", in terms of power production, in the presence of longer waves which are typically more frequent during more energetic sea states. This concept is shown in Fig. 2, where idealized simulations of 3 different point absorbers with diameters of 9, 12 and 22.5 m, and respective mass of 70000, 175000 and 280000 kg is presented. Here is possible to observe how the peak of the estimated production, with constant wave height of 1 m, is shifted towards longer periods as the size (and mass) of the device increases. It is also possible to verify the effect of including the sub-optimal PTO control in the WEC response simulation (dashed lines) or using a fixed PTO value (continuous lines).

Three different point absorbers' farms are proposed to eval-

uate the effects of multi-size arrays in terms of mean produced power (compared to single-size ones). All cases consider 10 devices arranged in a pyramidal, layout with 2 different diameters and mass used in the case of multi-size farms. The size and mass specifications are presented Fig. 3. Note that for all cases, the distance between the center of the devices is kept constant with a value of $3\phi_1 = 27$ m (where $\phi_1 = 9$ m and $\phi_2 = 22.5$ m).

2.4 MREL wave hindcast

The 30 years wave dataset was generated at the Marine Renewable Energies Lab (MREL), using WW3 implemented with a regular multi-grid 2-way nesting system [29, 30]. The modelled domain covers the North Atlantic from latitudes 0.25° to 80° North with a spacial resolution of 0.25° (N_ATL-15M). Then, 2 nested grids with progressively higher resolution towards the European Atlantic waters are included: N_ATL-8M with a resolution of 0.125°, and the "coastal" grid EU-2M, with 0.03° of resolution (~ 2.3 km; see Fig. 4). For all grids, the spectrum is discretized using 36 exponentially spaced frequencies from 0.034 to 0.95 Hz, with a 1.1 increment factor from one frequency to the next. For the case of the spectral directional space, 24 discrete directions are considered for the North Atlantic grid N_ATL-15M (resolution of 15°), and 36 directions for N_ATL-8M and EU-2M (resolution of 10°).

To force the model, the following fields have been considered:

- ERA5 winds [31] for wave generation. Wind fields are applied to all grids.
- COPERNICUS-GLOBCURRENT surface global (quasi-geostrophic) currents (CMEMS product MULTIOBS_GLO_PHY_REP_015_004) which are applied applied only in N_ATL-15M.
- The ice concentration from Ifremer SSMI-derived product [32] considering a 1 m constant thickness. This forcing is applied in all grids.
- Tidal levels and currents taken from the Atlantic-European North West Shelf-Ocean Physics Reanalysis (CMEMS product NWSHELF_MULTIYEAR_PHY_004_009). In this case, currents are applied in N_ATL-8M and EU-3M, but tidal levels are use only in EU-3M were shallower regions with large tidal ranges are better resolved.

The included parameterizations for wind input and wave dissipation are taken from the ST4 source terms package developed by Ardhuin et al. [33]. Further adjustments were applied to the swell dissipation term from the ocean-atmosphere interactions parameterization [33], following the methodology described in [34]. These modifications are mainly aimed to improve the wave heights distributions and reduce the overall biases in the North-East Atlantic. In addition, to partially mitigate the known underestimation of ERA5 high wind intensities [34, 35], a slight correction was applied to the input wind speeds > 20.5 m/s (see equation 6 in [34]).

The Discrete Interaction Approximation [DIA; 36] is used to represent the 4-wave nonlinear interactions. Although this is a rather crude representation of the nonlinear interactions, the DIA allows to capture some of the main characteristics of the sea states which are relevant for wave energy applications : the peak period (T_p) and the significant wave height (H_s). These wave parameters are related to the position of the spectral energy peak and the overall energy contained in the spectrum respectively.

2.5 Analyzed locations

The proposed analysis is applied in 2 locations with different wave climate characteristics: Ireland (at the latitude of Doonbeg), and off the coast of The Netherlands (North of the Frisian Islands). The Atlantic coast of Ireland is exposed to long swells and energetic storms during winter. On the other hand, The coast of the Netherlands is located in the Southern end of the North Sea, where the influence of swells form the North Atlantic is very low and the wave climate is dominated by local winds. The analyzed locations off the coast of Ireland and The Netherlands are identified as IRE and NED respectively. The coordinates and depths of these locations are specified in Fig. 5.

3. RESULTS

3.1 Sea states characteristics at the analyzed locations

As mentioned earlier, the wave climate (and depth) characteristics at IRE and NED are very different. Here the $H_s - T_p$ bi-variate distribution is computed using 30 years of wave data taken from the MREL-Hindcast. In Fig. 6 is possible to observe that most frequent $H_s - T_p$ combinations in IRE are concentrated between wave heights of 1.5 to 2.5 m and periods of 8 to 12 s. At NED, the most frequent occurrences are concentrated in the wave heights' range of 1 to 2 m and periods of 4 to 6 s, considerably shorter waves compared to those of the North Atlantic. The T_p histograms provide further information on the wave climate characteristics and an idea on how important is the presence of longer wave components outside the most frequent wave conditions. At IRE there is a clear second peak of T_p occurrences at 14 s, in average 4 s away from the range of most frequent periods (between 8 and 10 s). On the other hand, at NED there are 2 well defined peaks of T_p occurrences, but these are only 2 s away, with the first peak at 6 s and the second one at 8 s.

This analysis could be further refined by including seasonality and/or a POT type analysis to identify the occurrences of stronger sea sates. For now, the bulk of the data already provides a good idea of the presence of sea states with longer periods outside the most frequent conditions. This is specially clear at IRE, with an estimated cumulative occurrence of 15.5% of sea states with T_p in the reange of 13 to 15 s. It should be noticed that this range of periods matches the one for peak power absorption/production for a single WEC with a diameter of 22.5 m and 280000 kg of mass (see Fig. 2).

3.2 Produced power estimations

The power matrices at IRE and NED were derived using the average of the corresponding spectra from each $H_s - T_p$ combination assigned at a given bin range. With this approach it is expected to better represent the mean sea state conditions related to every H_s-T_p bin and thus, improve the estimation of the WECs dynamic response. In Fig. 7 an example of the different power matrices obtained at IRE and NED with a single-size WEC array

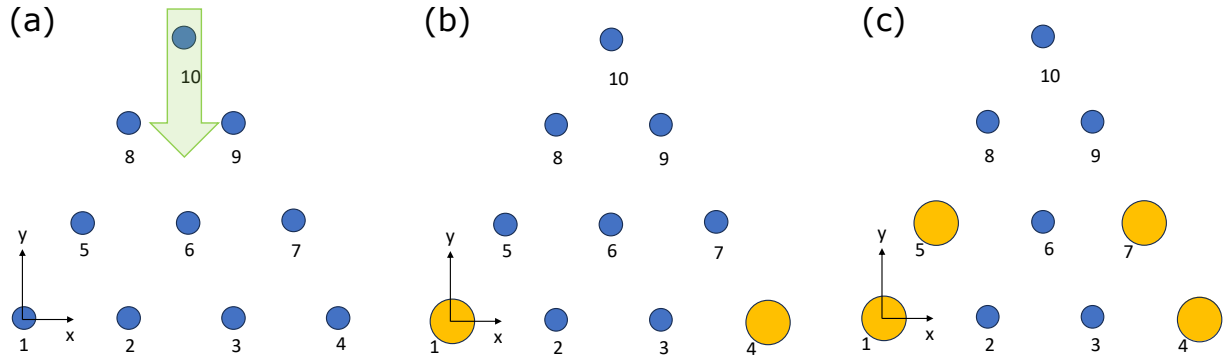

FIGURE 3: Analyzed WEC farms layouts. (a) Case 1: Single size $10\phi_1$ array WEC array. (b) Case 2: $8\phi_1$-$2\phi_2$ multi size array. (c) Case 3: $6\phi_1$-$4\phi_2$ multi size array. In blue, WECs with diameter $\phi_1 = 9$ m and total mass of 70000 kg. In orange, WECs with diameter $\phi_2 = 22.5$ m and total mass of 280000 kg. Green arrow shows the considered wave incidence for all simulations (cases). Distance between devices in all cases is $3\phi_1 = 27$ m.

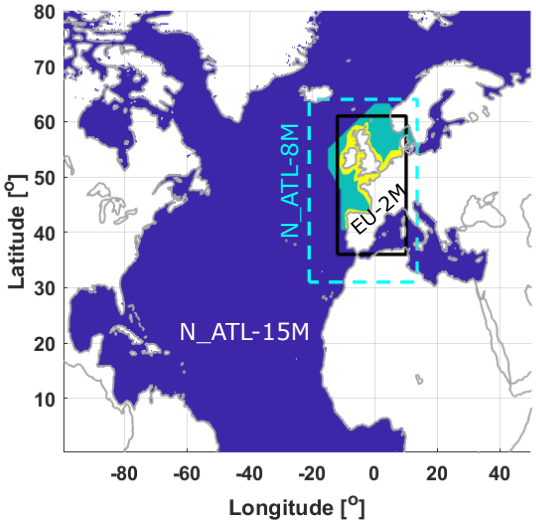

FIGURE 4: Multi-grid 2-way nesting setup used in WW3. Active N_ATL-15M grid nodes in dark blue, active nodes from N_ATL-8M grid in green , in yellow active nodes from the high resolution EU-2M grid. Figure taken from [26].

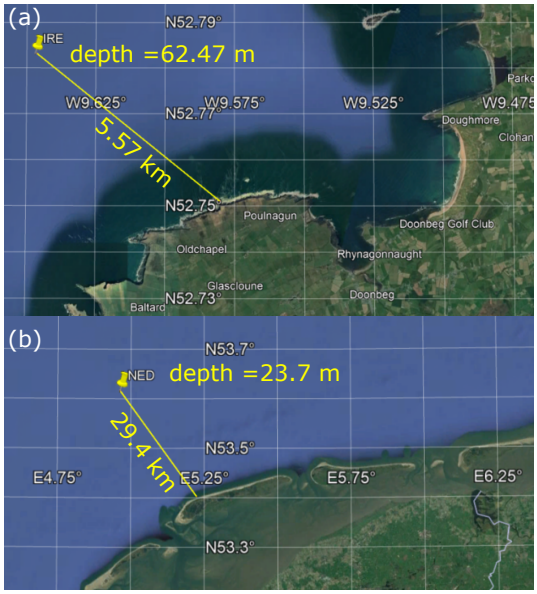

FIGURE 5: Analyzed locations. (a) Ireland (IRE), longitude −9.64°, latitude 52.78°. (b) The Netherlands (NED), longitude 4.96°, latitude 53.61°. Specified depth is with respect to the mean sea level. Map data are from ©Google Landast / Copernicus.

$10\phi_1$ and the proposed multi-size array $8\phi_1$-$2\phi_2$ (see Fig. 3 for details). A summary on the different power productions estimated from all cases is presented in Table 2. Note that a cap for wave heights larger than 9 m has been applied to consider the standard operation range of point absorbers.

In Fig. 7.a is possible to see that the highest power absortion/production for a 10 single-size WEC array falls within the 8 to 12 second T_p range, similar to the theoretical example shown in Fig. 2 for a single WEC. Once 2 larger devices are added to the array (case $8\phi_1$-$2\phi_2$;Fig. 7.a mid panel), the production peak clearly shifts to he range of 14.4 to 17 s. In fact, adding larger devices not only affects the increase of production for larger periods, there is also an overlap of the effect of the bigger devices to shorter periods too (Fig. 7.a right panel). It is interesting to see that, by including 2 larger devices, it is already possible to double the estimated absorbed power for approximately all periods > 6 s.

The estimation of the yearly mean produced power at IRE, shows a large 140% increase in the production with $8\phi_1$-$2\phi_2$ compared to $10\phi_1$ and a 320% increase with $6\phi_1$-$4\phi_2$ (see Table 2).

Given the reduced depth conditions at NED, it is not realistic to analyze cases $8\phi_1$-$2\phi_2$ and $6\phi_1$-$4\phi_2$ with $\phi_2 = 22.5$ m. Instead, a diameter $\phi_2 = 12$ m with a mass of 175000 kg is selected to verify the overall increase of power production. As seen in Fig. 2, the devices with with 9 and 12 m of diameter have only a slight different period shift in their peak response, but the point absorber with 12 m diameter (with PTO control) presents almost a constant 50% increase in the absorbed power for periods between 8 to 25 s. Although not exactly the same, this behavior is also observed in the power matrix of the $8\phi_1$-$2\phi_2$ WEC array in Fig. 7.b. By only including 2 slightly larger WECs there is a ~40% increase in the absorbed/produced power in almost all

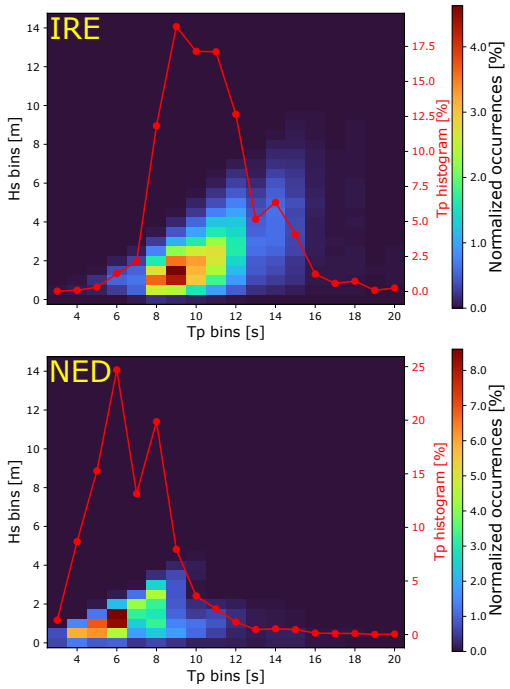

FIGURE 6: $H_s - T_p$ bi-variate distribution and T_p histogram computed at IRE (top panel) and NED (bottom panel) using 30 years of wave data.

$H_s - T_p$ combinations for wave heights ranging from 3 to 9 m and periods from 10 to 20 s (Fig. 7.b, right panel). This suggest a potential economical benefit in using multi-size WEC farms, allowing higher production rates. In this case, The estimation of the yearly mean produced power at NED, shows a non negligible 20% increase in the production with $8\phi_1$-$2\phi_2$ compared to $10\phi_1$.

4. CONCLUSIONS

The main objective of the study was to quantity the differences in the produced power of multi-size WEC farms compared to the commonly analyzed single-size arrays. The aim of using different WEC sizes is to improve the produced power during the occurrence of stronger sea states, outside the most frequent wave conditions at a specific location. The simulation of point absorbers' farms was done using the boundary element model HAMS-MREL. On the other hand, the input wave data was taken from the MREL-Hindcast, created using WW3 and specially tuned for the North Altantic European waters.

The differences between the proposed arrays were analyzed in terms of the changes in the power matrices obtained for multi-size WEC arrays, compared to single-size ones of 9 m diameter. Furthermore, the analysis is completed by comparing the yearly mean produced power for each proposed WEC farm case: $10\phi_1$, $8\phi_1$-$2\phi_2$, and $6\phi_1$-$4\phi_2$. This was done for 2 selected locations with different wave climate and depth conditions IRE (Ireland) and NED (The Netherlands).

Preliminary results point to a significant increase in the absorbed/produced power when only 2 larger devices are considered in a 10 WECs pyramidal array. Particularly at IRE, the inclusion

TABLE 2: Produced power estimations. ϕ_2 is 22.5 and 12 m for IRE and NED respectively.Produced power is assumed equal to absorbed power (no losses).

Location	Case	Yearly mean production [MW hr]	30 years production [MW hr]
IRE	10ϕ	10518.8	315565.8
IRE	$8\phi_1$-$2\phi_2$	25961.4	778844.1
IRE	$6\phi_1$-$4\phi_2$	44531.4	1335941.7
NED	10ϕ	2547.7	76431.1
NED	$8\phi_1$-$2\phi_2$	3220.4	96612.7
NED	$6\phi_1$-$4\phi_2$	4102.3	123067.9

of 2 WECs with 22.5 m diameter and 280000 kg helps to increase the yearly mean power production by about 140%. Although the larger devices were "tuned" to perform better in the neighborhood of 15 s, their inclusion has an effect across a wide range of wave periods.

A somewhat different test was performed at NED, where the multi-size arrays were simulated including a slightly bigger device of 12 m (175000 kg). In this case an increase of 20% and 61% was obtained in the yearly mean production when respectively 2 or 4 larger devices are included in the array. This results represent an interesting finding as there is a potential economical benefit in the inclusion of a few slightly bigger devices in the array. Although outside the scope of this paper, adding slightly larger devices to the array may partly solve destructive behavior (in WECs interactions) in farms bounded to a small available surface. Distance between arrays is of importance since the radiated waves from the WECs can create a destructive superposition with some components (frequencies) from the incoming wave field. If that is the case, a reduction in the absorbed power is observed. It is always possible that the available space for deployment can be reduced and the optimal spacing of the devices, to avoid destructive interference of some wave components, cannot be achieved. Thus, including WECs with larger size/mass can help to compensate for the potential loss in production.

It is expected that with a more detailed study of the local sea states characteristics it will be possible to find a refined relationship between the "small" to "larger" devices in the WEC farm design. The characterization of the resource could be done including seasonality or a peaks over threshold type analysis. This multi-size design approach, specially adjusted to local wave climate and using passive controls, might have a positive economical impact. It is thought that stretching the power production efficiency towards longer periods will be beneficial for a more even production throughout the year, with a partial reduction of the operation downtime effects. These are subjects of ongoing research, including the proper estimations of the CAPEX and OPEX for multi-size WEC arrays.

ACKNOWLEDGMENTS

This work is part of the EU-SCORES project that has received funding from the European Union's Horizon 2020 research and innovation programme under grant agreement No

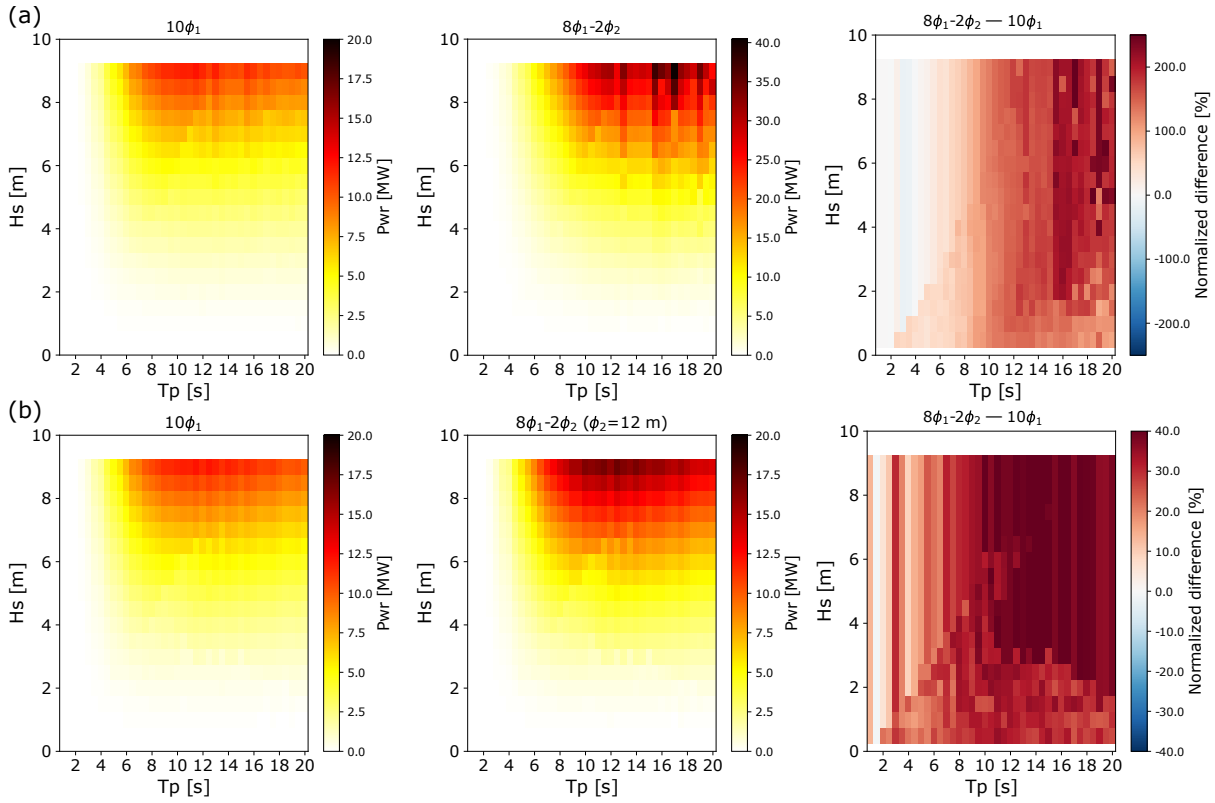

FIGURE 7: Example of power matrices and normalized differences between single and multi-size WEC arrays ($8\phi_1$-$2\phi_2$ - $10\phi_1$) for (a) IRE and (b) NED locations. On left panel results for single-size $10\phi_1$ array , on mid panel $8\phi_1$-$2\phi_2$ multi-size array, normalized difference with respect to $10\phi_1$.

101036457. The authors would like to thank to the anonymous reviewers for their valuable input that helped to improve the content of this paper.

REFERENCES

[1] Gunn, Kester and Stock-Williams, Clym. "Quantifying the global wave power resource." *Renewable energy* Vol. 44 (2012): pp. 296–304. DOI https://doi.org/10.1016/j.renene.2012.01.101.

[2] Li, Ning, García-Medina, Gabriel, Cheung, Kwok Fai and Yang, Zhaoqing. "Wave energy resources assessment for the multi-modal sea state of Hawaii." *Renewable Energy* Vol. 174 (2021): pp. 1036–1055.

[3] Guillou, Nicolas, Lavidas, George and Chapalain, Georges. "Wave energy resource assessment for exploitation—a review." *Journal of Marine Science and Engineering* Vol. 8 No. 9 (2020): p. 705. DOI https://doi.org/10.3390/jmse8090705.

[4] Ribal, Agustinus, Babanin, Alexander V, Zieger, Stefan and Liu, Qingxiang. "A high-resolution wave energy resource assessment of Indonesia." *Renewable Energy* Vol. 160 (2020): pp. 1349–1363. DOI https://doi.org/10.1016/j.renene.2020.06.017.

[5] Besio, G, Mentaschi, L and Mazzino, A. "Wave energy resource assessment in the Mediterranean Sea on the basis of a 35-year hindcast." *Energy* Vol. 94 (2016): pp. 50–63.

[6] van Nieuwkoop, Joana CC, Smith, Helen CM, Smith, George H and Johanning, Lars. "Wave resource assessment along the Cornish coast (UK) from a 23-year hindcast dataset validated against buoy measurements." *Renewable energy* Vol. 58 (2013): pp. 1–14. DOI https://doi.org/10.1016/j.renene.2013.02.033.

[7] Lavidas, George and Venugopal, Vengatesan. "Application of numerical wave models at European coastlines : A review." *Renewable and Sustainable Energy Reviews* Vol. 92 (2018): pp. 489–500. DOI 10.1016/j.rser.2018.04.112. URL https://doi.org/10.1016/j.rser.2018.04.112.

[8] Mwasilu, Francis and Jung, Jin-Woo. "Potential for power generation from ocean wave renewable energy source: a comprehensive review on state-of-the-art technology and future prospects." *IET Renewable Power Generation* Vol. 13 No. 3 (2019): pp. 363–375. DOI https://doi.org/10.1049/iet-rpg.2018.5456.

[9] Wu, Zang and Viola, Alessia. "The challenge of wave energy: A review of the WECs state of the art developed in the world." *OCEANS 2017-Aberdeen* (2017): pp. 1–6DOI 10.1109/OCEANSE.2017.8084980.

[10] Babarit, Aurélien, Hals, Jorgen, Muliawan, Made Jaya, Kurniawan, Adi, Moan, Torgeir and Krokstad, Jorgen. "Numerical benchmarking study of a selection of wave energy converters." *Renewable energy* Vol. 41 (2012): pp. 44–63. DOI https://doi.org/10.1016/j.renene.2011.10.002.

[11] Falcao, Antonio F de O. "Wave energy utilization: A review of the technologies." *Renewable and sustainable energy reviews* Vol. 14 No. 3 (2010): pp. 899–918. DOI https://doi.org/10.1016/j.rser.2009.11.003.

[12] Göteman, Malin, Engström, Jens, Eriksson, Mikael and Isberg, Jan. "Optimizing wave energy parks with over 1000 interacting point-absorbers using an approximate analytical method." *International Journal of Marine Energy* Vol. 10 (2015): pp. 113–126. DOI http://dx.doi.org/10.1016/j.ijome.2015.02.001.

[13] Astariz, Sharay and Iglesias, Gregório. "The economics of wave energy: A review." *Renewable and Sustainable Energy Reviews* Vol. 45 (2015): pp. 397–408. DOI https://doi.org/10.1016/j.rser.2015.01.061.

[14] Son, Daewoong and Yeung, Ronald W. "Optimizing ocean-wave energy extraction of a dual coaxial-cylinder WEC using nonlinear model predictive control." *Applied energy* Vol. 187 (2017): pp. 746–757. DOI https://doi.org/10.1016/j.apenergy.2016.11.068.

[15] Wang, Liguo and Isberg, Jan. "Nonlinear passive control of a wave energy converter subject to constraints in irregular waves." *Energies* Vol. 8 No. 7 (2015): pp. 6528–6542. DOI https://doi.org/10.3390/en8076528.

[16] de la Villa Jaén, Antonio, Andrade, Dan El Montoya and García Santana, Agustín. "Increasing the efficiency of the passive loading strategy for wave energy conversion." *Journal of Renewable and Sustainable Energy* Vol. 5 No. 5 (2013): p. 053132. DOI https://doi.org/10.1063/1.4824416.

[17] Oskamp, Jeffrey A and Özkan-Haller, H Tuba. "Power calculations for a passively tuned point absorber wave energy converter on the Oregon coast." *Renewable Energy* Vol. 45 (2012): pp. 72–77. DOI https://doi.org/10.3390/en8076528.

[18] Hals, Jørgen, Falnes, Johannes and Moan, Torgeir. "A Comparison of Selected Strategies for Adaptive Control of Wave Energy Converters." *Journal of Offshore Mechanics and Arctic Engineering* Vol. 133 No. 3 (2011): p. 031101. DOI 10.1115/1.4002735. URL https://doi.org/10.1115/1.4002735.

[19] The WAVEWATCH III ® Development Group. "User manual and system documentation of WAVEWATCH III ® version 6.07." Tech. Note 333. NOAA/NWS/NCEP/MMAB, College Park, MD, USA. 2019. 465 pp. + Appendices.

[20] Tolman, H. L. "The numerical model WAVEWATCH: a third generation model for hindcasting of wind waves on tides in shelf seas." Technical Report No. 89-2. Faculty of civil engineering, Delft University of Technology. 1989. ISSN 0169-6548.

[21] "Corpower." (2023). URL https://corpowerocean.com/wave-energy-technology/.

[22] Hals, Jorgen, Ásgeirsson, Gunnar Steinn, Hjálmarsson, Eysteinn, Maillet, Jéromine, Möller, Patrik, Guérinel, Matthieu and Lopes, Miguel. "Tank testing of an inherently phase-controlled wave energy converter." *International Journal of Marine Energy* Vol. 15 (2016): pp. 68–84. DOI https://doi.org/10.1016/j.ijome.2016.04.007. URL https://www.sciencedirect.com/science/article/pii/S2214166916300182. Selected Papers from the European Wave and Tidal Energy Conference 2015, Nantes, France.

[23] Hals, Jorgen, Bjarte-Larsson, Torkel and Falnes, Johannes. "Optimum Reactive Control and Control by Latching of a Wave-Absorbing Semisubmerged Heaving Sphere." Vol. 21st International Conference on Offshore Mechanics and Arctic Engineering, Volume 4 (2002): pp. 415–423. DOI 10.1115/OMAE2002-28172. URL https://asmedigitalcollection.asme.org/OMAE/proceedings-pdf/OMAE2002/36142/415/4545242/415_1.pdf, URL https://doi.org/10.1115/OMAE2002-28172.

[24] Alves, M. "Chapter 2 - Frequency-Domain Models." Folley, Matt (ed.). *Numerical Modelling of Wave Energy Converters*. Academic Press (2016): pp. 11–30. DOI https://doi.org/10.1016/B978-0-12-803210-7.00002-5. URL https://www.sciencedirect.com/science/article/pii/B9780128032107000025.

[25] Liu, Yingyi. "HAMS: A Frequency-Domain Preprocessor for Wave-Structure Interactions—Theory, Development, and Application." *Journal of Marine Science and Engineering* Vol. 7 No. 3 (2019). DOI 10.3390/jmse7030081. URL https://www.mdpi.com/2077-1312/7/3/81.

[26] Alday, Matías, Raghavan, Vaibhav and Lavidas, George. "Analysis of the North Atlantic offshore energy flux from different reanalysis and hindcasts." *Proceedings of the 15th European Wave and Tidal Energy Conference (EWTEC), 3–7 September 2023, Bilbao*. 2023. DOI https://doi.org/10.36688/ewtec-2023-140.

[27] Malta, Edgard B., Gonc¸alves, Rodolfo T., Matsumoto, Fabio T., Pereira, Felipe R., Fujarra, Andre´ L. C. and Nishimoto, Kazuo. "Damping Coefficient Analyses for Floating Offshore Structures." Vol. 29th International Conference on Ocean, Offshore and Arctic Engineering: Volume 1 (2010): pp. 83–89. URL https://doi.org/10.1115/OMAE2010-20093.

[28] Folley, M. and Whittaker, T. "Spectral modelling of wave energy converters." *Coastal Engineering* Vol. 57 No. 10 (2010): pp. 892–897. DOI https://doi.org/10.1016/j.coastaleng.2010.05.007. URL https://www.sciencedirect.com/science/article/pii/S0378383910000700.

[29] Tolman, Hendrik L. "A mosaic approach to wind wave modeling." *Ocean Modelling* Vol. 25 (2008): pp. 35–47. DOI 10.1016/j.ocemod.2008.06.005.

[30] Chawla, Arun, Tolman, Hendrik L., Gerald, Vera, Spindler, Deanna, Spindler, Todd, Alves, Jose-Henrique G. M., Cao, Degui, Hanson, Jeffrey L. and Devaliere, Eve-Marie. "A Multigrid Wave Forecasting Model: A New Paradigm in Operational Wave Forecasting." *Weather and Forecasting* Vol. 28 (2013): pp. 1057–1078. DOI 10.1175/waf-d-12-00007.1.

[31] Hersbach, Hans, Bell, Bill, Berrisford, Paul, Hirahara, Shoji, Horányi, András, Muñoz-Sabater, Joaquín, Nicolas, Julien, Peubey, Carole, Radu, Raluca, Schepers, Dinand et al. "The ERA5 global reanalysis." *Quarterly Journal of*

the Royal Meteorological Society Vol. 146 No. 730 (2020): pp. 1999–2049. DOI 10.1002/qj.3803.

[32] Girard-Ardhuin, F. and Ezraty, R. "Enhanced Arctic sea ice drift estimation merging radiometer and scatterometer data." *IEEE Transactions on Geoscience and Remote Sensing* Vol. 50 (2012): pp. 2639–2648. DOI 10.1109/TGRS.2012.2184124.

[33] Ardhuin, Fabrice, Rogers, Erick, Babanin, Alexander, Filipot, Jean-François, Magne, Rudy, Roland, Aron, van der Westhuysen, Andre, Queffeulou, Pierre, Lefevre, Jean-Michel, Aouf, Lotfi and Collard, Fabrice. "Semi-empirical dissipation source functions for wind-wave models: part I, definition, calibration and validation." *Journal of Physical Oceanography* Vol. 40 No. 9 (2010): pp. 1917–1941. DOI 10.1175/2010JPO4324.1.

[34] Alday, Matias, Accensi, Mickael, Ardhuin, Fabrice and Dodet, Guillaume. "A global wave parameter database for geophysical applications. Part 3: Improved forcing and spectral resolution." *Ocean Modelling* Vol. 166 (2021): p. 101848. DOI https://doi.org/10.1016/j.ocemod.2021.101848.

[35] Pineau-Guillou, L., Ardhuin, F., Bouin, M.-N., Redelsperger, J.-L., Chapron, B., Bidlot, J.R. and Quilfen, Y. "Strong winds in a coupled wave-atmosphere model during a North Atlantic storm event: evaluation against observations." *Quart. Journ. Roy. Meteorol. Soc.* Vol. 144 (2018): pp. 317–332. DOI 10.1002/qj.3205.

[36] Hasselmann, S. and Hasselmann, K. "Computation and parameterizations of the nonlinear energy transfer in a gravity-wave spectrum. Part I: a new method for efficient computations of the exact nonlinear transfer." *Journal of Physical Oceanography* Vol. 15 (1985): pp. 1369–1377. DOI 10.1175/1520-0485(1985)015<1369:CAPOTN>2.0.CO;2.